Manual dexterity in Neanderthals

These primitive people may have been as handy with their tools as modern humans are.

Despite their ability to make and use stone tools, Neanderthals were presumed to have had limited manual dexterity on the basis of the anatomy of their thumb and forefinger[1] — a contention that has been called into question[2–4]. Here we investigate the likely extent of Neanderthal thumb function by using a three-dimensional dynamic simulation that is based on the anatomical details and articular morphology of the thumb and index finger. We find that these digits could make tip-to-tip contact, and conclude that manual dexterity in Neanderthals was probably not significantly different from that of modern humans.

Epoxy casts of the La Ferrassie I Neanderthal thumb and index-finger bones were scanned with a Minolta Vivid 900 laser digitizer to produce three-dimensional polygon mesh models that are accurate to within ±20 micrometres (Fig. 1a, b). We used these bone models to generate an articulated computer model with Maya Unlimited software. Movements were simulated by user-assigned ranges of motion at the centre of rotation of each joint with the aid of Maya animation tools.

A saddle-shaped metacarpal-1 base is a key feature for the production of precision grips (that is, the pads of the thumb and the fingers are opposed)[5]. A three-dimensional morphometric analysis indicates that some Neanderthal metacarpal-1 bases approach a condyloid shape because they lack a highly developed palmar beak[4]. The La Ferrassie I metacarpal-1 base has a moderately developed palmar beak that is at the extreme of the modern-human range of variation[4], making it likely that the range of movements of its trapezial–metacarpal joint is similar to that of modern humans.

In fact, given the open configuration of the Neanderthal trapezial–metacarpal-1 joint, all Neanderthal thumbs were probably more mobile than that of modern humans. But as it has been suggested that Neanderthal thumb movements were restricted[1,6,7], we minimized the mobility of the thumb by using the middle range of published modern-human flexion/extension values[5,8] and by eliminating metacarpal-1 pronation entirely.

The movement of the index finger is another important factor for producing precision grips. The asymmetry of the second metacarpal head (one half of the index-finger knuckle joint), combined with actions of muscle contraction and joint ligaments, causes the finger to turn towards the thumb in full flexion[9]. Although Neanderthal metacarpal-2 heads are slightly less asymmetrical than those of modern humans[4], we were again cautious and restricted movement at the metacarpophalangeal joint to flexion/extension only. We assigned published modern-human flexion/extension values to the interphalangeal joints[9] because these joints are functionally equivalent in Neanderthals and modern humans.

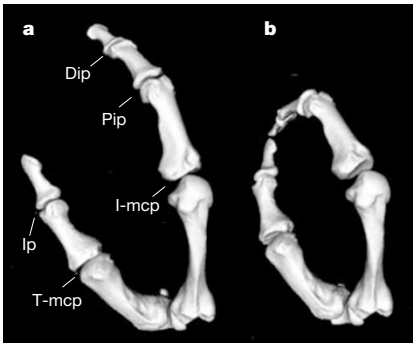

Figure 1 The laser-scanned Neanderthal La Ferrassie I thumb and index finger. **a, b,** Dorsal views of the thumb (left) and index finger (right) in **a**, their neutral position, and **b**, the fully flexed position. In **b**, the two digits make tip-to-tip contact; the thumb carpometacarpal (bottom) joint is flexed by 10° from its neutral position, the thumb metacarpophalangeal (T-mcp) joint is flexed by 35°, the interphalangeal (Ip) joint is flexed by 15°, the index-finger metacarpophalangeal (I-mcp) joint is flexed by 45°, the proximal interphalangeal (Pip) joint is flexed by 65°, and the distal interphalangeal (Dip) joint is flexed by 15°.

Even allowing for significantly limited joint movements relative to modern humans, flexion of the thumb and index finger results in tip-to-tip contact (Fig. 1b). Musgrave[1] suggested that the Neanderthal's short thumb and first-finger proximal phalanges could have inhibited their precision of movement, but our results indicate that this is not the case. As there is no significant difference between Neanderthals and modern humans in the locations of their muscle and ligamentous attachments[2], there remains no anatomical argument that precludes modern-human-like movement of the thumb and index finger in Neanderthals.

The demise of the Neanderthals cannot be attributed to any physical inability to use or manufacture Upper-Palaeolithic-like (Châtelperronian) tools, as the anatomical evidence presented here and the archaeological evidence[10] both indicate that they were capable of manufacturing and handling such implements.

Wesley A. Niewoehner*, Aaron Bergstrom†, Derrick Eichele†, Melissa Zuroff†, Jeffrey T. Clark†

**Department of Anthropology, California State University, San Bernardino, California 92407, USA*
e-mail: wniewoeh@csusb.edu
†Archaeology Technologies Lab, North Dakota State University, Fargo, North Dakota 58105, USA

1. Musgrave, J. H. *Nature* **233,** 538–541 (1971).
2. Trinkaus, E. *The Shanidar Neandertals* (Academic, New York, 1983).
3. Niewoehner, W. A., Weaver, A. & Trinkaus, E. *Am. J. Phys. Anthropol.* **103,** 219–233 (1997).
4. Niewoehner, W. A. *The Functional Anatomy of Late Pleistocene and Recent Human Carpometacarpal and Metacarpophalangeal Articulations* (Univ. New Mexico Press, Albuquerque, 2000).
5. Cooney, W., Lucca, M. J., Chao, E. Y. S. & Linscheid, R. *J. Bone Joint Surg. Am.* **63** A, 1371–1381 (1981).
6. Boule, M. *Ann. Paleontol.* **6,** 111–172; **7,** 21–56, 85–192; **8,** 1–70 (1911–1913); republished by Masson, France (1913).
7. Vlcek, E. *Bull. Mém. Soc. Anthropol. Paris* **13,** 257–276 (1975).
8. Kraemer, B. A. & Gilula, L. A. in *The Traumatized Hand and Wrist* (ed. Gilula, L. A.) 65–92 (Saunders, Philadelphia, 1992).
9. Craig, S. M. *Hand Clin.* **8,** 693–700 (1992).
10. Churchill, S. E. & Smith, F. *Yearbook Phys. Anthropol.* **43,** 61–115 (2000).

Competing financial interests: declared none.

Wetting properties

When larger drops evaporate faster

In an ensemble of volatile liquid drops, either in suspension or on a partially wetted substrate, large drops grow at the expense of smaller ones when the pressure is just above the saturated-vapour pressure. Below this critical pressure, all drops evaporate, with the smallest drops evaporating fastest. But an array of water drops of different sizes on a mica substrate cleaved in a vacuum behave differently: below the equilibrium vapour pressure, the largest drops evaporate fastest and the smallest ones more slowly. Here we show that this behaviour is related to the coexistence of thick and thin water films during evaporation.

An evaporating water film on mica breaks into interesting patterns that have been predicted theoretically[1,2] and have been shown experimentally to result from competing van der Waals and polar surface forces between the water and the substrate[3,4], with spreading pressures S^{VW} and S^{P}, respectively. The excess Gibbs free energy per unit area has been described as a function of thickness[3,5,6], as $g(h) = S^{VW}d_0^2/h^2 + S^{P}\exp[(d_0 - h)/l]$, where l is a screening length and d_0 is the molecular diameter.

The resulting interaction potential can have minima at two different film thicknesses, corresponding to molecularly thin and macroscopically thick films. Phase equilibrium between the two films and the

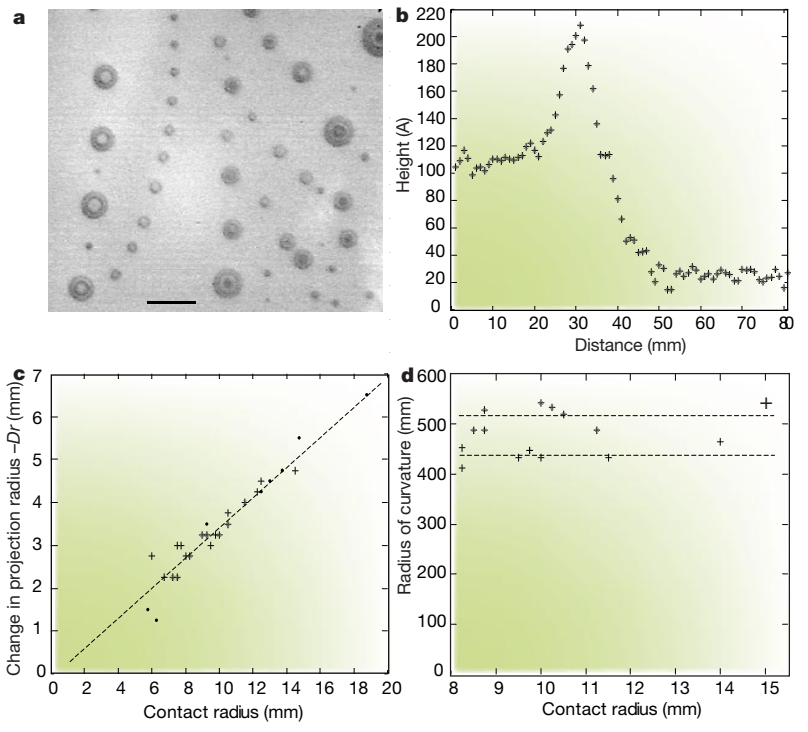

Figure 1 Behaviour of evaporating water drops on a cleaved mica substrate. **a,** An array of water drops of widely differing sizes at 0 °C, photographed at $\lambda = 546$ nm using interference contrast. The first dark ring appears at a thickness of 111 nm. Scale bar, 100 μm. **b,** Profile of the interface between the thin and thick films, measured by three-beam interferometry, involving reflections at the vapour–film interface and both mica surfaces. **c,** Change in projection radius of drops during 15 min as a function of their radius, for three different experiments under the same conditions, $p/p_{sat} = 0.920 \pm 0.002$. For comparison, on a partially wetted substrate, under the same p/p_{sat}, small drops were swallowed by big ones within 30 s. **d,** The radius of curvature of drops is independent of their projection radius. The two lines refer to the same field of drops at different times. Typical error bar is shown on one point.

vapour, corresponding to a Maxwell construction on the chemical potential $\mu_{film} = \rho_{liq}^{-1} dg/dh$, is similar to that between a liquid and a solid, for example, and a first-order phase transition occurs between them.

The remarkable dendrite-like patterns that develop during evaporation have been shown[4] to mimic two-dimensional diffusion-limited solidification[7,8]. The late-stage pattern consists of an array of slowly evaporating water drops of widely differing sizes (Fig. 1a). Then, if the contact angle is constant, coarsening[6,9] occurs, as in solidification or cooperative evaporation[10], in which larger drops acquire fluid from smaller ones through vapour transport. A drop with a smaller radius of contact with the substrate has a smaller radius of curvature, R, and must therefore evaporate faster owing to the Gibbs–Thomson contribution, $2\gamma/R$, to its vapour pressure, where γ is the surface tension.

Instead, we have observed that all of the drops continue to evaporate together, the smaller ones even evaporating more slowly than the larger ones. We attribute this behaviour to the thin, continuous film of water that connects the drops. Figure 1b shows experimental measurements of the thickness of the two films predicted by this model. The two films are separated by a hydrodynamic rim, which has previously been seen both in simulations[3] and in experiments[4,11]. The measurements used a new form of three-beam interferometry (see legend to Fig. 1b).

For the case investigated, the two films have thicknesses of 25 ± 5 and 110 ± 10 Å. The drops, with their free surfaces far from the substrate, have excess chemical potential $2\rho_{liq}^{-1}\gamma/R$. For equilibrium with the continuous thin film, R must therefore be the same for all the drops. This implies that the contact angle increases with a contact radius. But because the film is continuous, the meeting between liquid, vapour and substrate, which defines the edge of a drop, is not present, and so a conventional contact angle cannot be defined.

It was found in simulations[12] that the contact angle of a drop increases with its volume. Water evaporating from the spherical cap is compensated for by contraction of the contact radius, r, at velocity $v = -dr/dt$. A balance of volumes gives $2\pi r v(h_2 - h_1) = 2\alpha\rho_{liq}^{-1}\pi r^2\gamma/R$, where α is the evaporation parameter[4]. As R is the same for all drops, it can be shown that dr/dt is proportional to $-r$, as has been confirmed experimentally (Fig. 1c, d). The typical situation, in which large drops in an array grow at the expense of the smaller ones, is therefore not universally observed, and when the drops coexist with a microscopically thin continuous surface layer, they behave differently.

I. Leizerson*, S. G. Lipson*, A. V. Lyushnin†
**Department of Physics, Technion-Israel Institute of Technology, 32000 Haifa, Israel*
e-mail: philya@techunix.technion.ac.il
†Department of Theoretical Physics, Perm State Pedagogical University, Perm 614600, Russia

1. Cazabat, A.-M. *Contemp. Phys.* **28,** 347–364 (1987).
2. Brochard-Wyart, F. *Soft Matter Physics* 7–44 (Springer, Berlin, 1995).
3. Sharma, A. & Jameel, A. *J. Colloid Interface Sci.* **161,** 190–208 (1993).
4. Samid-Merzel, N., Lipson, S. G. & Tanhauser, D. S. *Phys. Rev. E* **57,** 2906–2913 (1998).
5. de Gennes, P. G. *Rev. Mod. Phys.* **57,** 325–359 (1985).
6. Israelachvili, J. *Intermolecular and Surface Forces* 2nd edn (Academic, San Diego, 1992).
7. Ben-Jacob, E. *Nature* **343,** 523–530 (1990).
8. Ihle, T. & Muller Krumbhaar, H. *Phys. Rev. Lett.* **70,** 3083–3086 (1993).
9. McHale, G., Rowan, S. M., Newton, M. I. & Banerjee, M. K. *J. Phys. Chem. B* **102,** 1964–1967 (1998).
10. Schafle, C., Bechinger, C., Rinn, B., David, C. & Leider, P. *Phys. Rev. Lett.* **83,** 5302–5305 (1999).
11. Elbaum, M. & Lipson, S. G. *Phys. Rev. Lett.* **72,** 3562–3565 (1994).
12. Sharma, A. *Langmuir* **9,** 3580–3586 (1993).

Competing financial interests: declared none.

Palaeobotany

Swimming sperm in an extinct Gondwanan plant

The now-extinct plant *Glossopteris* that dominated the Southern Hemisphere (Gondwana) during the Permian period serves as early evidence of continental drift[1,2], and may be ancestral to the group of seed plants known as angiosperms[3]. Here we describe a 250-million-year-old fossil from Homevale in Queensland, Australia, of anatomically preserved pollen tubes and swimming male gametes from *Glossopteris*. The discovery of this simple reproductive system in *Glossopteris* has implications for its phylogenetic relationships with extant groups of seed plants (conifers and flowering plants, for example) and for the evolution of pollination biology in general.

Five fossilized pollen tubes are evident in the pollen chamber of a single ovule, which has been attributed to *Glossopteris homevalensis*[2] (Fig. 1a, b). They are short and ovoid, unbranched, and contain gametes in several stages of development. Two of the pollen tubes contain a single, immature, spermatogenous cell, two of